Linear Analysis of Compressibility and Viscosity Effects on the MRT Instability in Z-pinch Implosions with Sheared Axial Flows [1]

Y. Zhang 1), N. Ding 1)

1) Institute of Applied Physics and Computational Mathematics, Beijing, China

e-mail contact of main author: zhang_yang@iapcm.ac.cn

Abstract. A linear analysis of the magneto-hydrodynamic stability of the Z-pinch plasma with axial flows is presented. The effects of compressibility, viscosity, and various profiles on the magneto-Rayleigh-Taylor instability are investigated respectively. Results indicate that, plasma compressibility plays an important role in the early stage of the implosion, and should be considered when estimating the growth rate. In the case without axial flows the effect of the viscosity seems nonsignificant, but the hybrid effect with the sheared flow should be calculated accurately if a sheared axial flow was present. The analysis of different axial flow profiles shows that, the mitigation effect of the axial flow on the MRT instability is caused by the radial velocity shear, and it is highly susceptible to the shear value nearby the plasma outer surface. By optimizing the flow profile, the mitigation performance can be promoted evidently.

1. Introduction

The electromagnetic implosions of Z pinches, which were used widely as an efficient and cost effective x-ray source to produce intense x-ray radiation[1,2], are highly susceptible to the magneto-Rayleigh-Taylor (MRT) instability, which results from the inward radial acceleration of the plasma by the magnetic field and develops rapidly during the imploding. Its development may destruct the cylindrical symmetry of the imploding shell before an equilibrium steady state is achieved and limit the stagnation densities and temperatures can be achieved. Therefore, mitigating this instability is important for optimizing the x-ray energy and power output.

Recently, the sheared axial flow (SAF) effect is demonstrated, both theoretically and experimentally, to be efficient on mitigating the m=0 and m=1 instabilities [3,4]. The results of the Zap Flow Z-pinch experiment at the University of Washington showed an axial velocity shear about $1.9\times10^{7}s^{-1}$ and a stable period of 17μs which is over 700 growth times.[5] Enlightened by these successes, Shumlak and Roderick begin to investigate its possible use of stabilizing the MRT instability in dynamic Z-pinch implosions.[6] Their analysis indicates that even a linear profile SAF can give a visible suppression on the development of MRT instability, especially to the short-wavelength modes. Such a stirring result excites us to make further analyze on the SAF effect to the Z-pinch implosions.

To make out a more precise estimation of the growth rate, the research should base on a relatively more generous model, which can describe the Z-pinch plasma more accurately. It is

[1] This work is supported by the National Natural Science Foundation of China (Project No. 10575014).

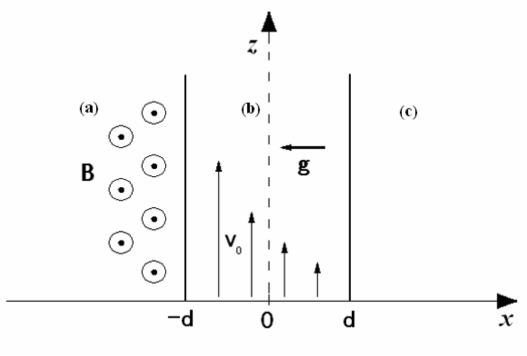

Fig. 1. The slab geometry used in the stability analysis.

well recognized that Z-pinch plasma is a compressible and viscous system, especially at the inward accelerating stage during which the MRT instability evolves most rapidly and the plasma temperature is relatively low. Results from the astrophysics researches suggests that the plasma compressibility has a tendency of reducing the growth rate of the Kelvin-Helmholtz (KH) instability, which will developed rapidly in the Z-pinch implosions as the SAF introduced.[7] In addition, the stabilizing effect of dynamic viscosity on the reversed-field pinch (RFP) also suggests the viscosity may play an important role in Z-pinch implosions too. Therefore, it's instructive to investigate the effects of compressibility and dynamic viscosity, which are expected to be helpful, on the stability in Z-pinch implosions with SAFs. The limitation of the realizable axial flows we can get presently in laboratories, probably about 1 Mach[8], also suggests that we should analyze the effects of various flow profiles to understand the mitigation mechanism of the axial sheared flow and make an optimization. The analyses of compressibility and dynamic viscosity are presented in Sec. 2 and Sec. 3 respectively. In Sec. 4 the numerical results of different flow profiles calculated with a relatively more generous model are shown and the stabilization mechanism of the axial sheared flow is discussed. At last, we make conclusions in Sec.5.

2. Effect of Compressibility

It is well recognized that an annular plasma implosion, particularly produced by a wire array, generates x-ray radiation more efficiently than a uniform gas puff implosion. Such an annular configuration can be replaced by a slab one while the shell thickness is sufficiently smaller than the pinch radius. Consider a plasma slab with a flow $\boldsymbol{v}_0$ and the effective inertia force acceleration $\boldsymbol{g}$ caused by a y-direction magnetic field and a z-direction current. All parameters vary in the x direction, except $\boldsymbol{g}$ which is constant. The Cartesian coordinate system used for the derivation was plotted in Fig. 1. The plasma mass continuity and motion equations, which include the plasma viscosity, are as follows,

$$\partial\rho/\partial t+\nabla\cdot(\rho\boldsymbol{v})=0, \tag{1}$$

$$\rho\partial\boldsymbol{v}/\partial t+\rho(\boldsymbol{v}\cdot\nabla)\boldsymbol{v}=\boldsymbol{J}\times\boldsymbol{B}+\nabla\cdot[\boldsymbol{\tau}]+\rho\boldsymbol{g}, \tag{2}$$

where all the notations are conventional, and $\nabla\cdot[\boldsymbol{\tau}]$ is the divergence of the stress-tensor including the plasma press and viscous stress. In this section, we neglect the viscosity effect to outstand the effect of compressibility, and the linearized equations become,

$$\partial \rho_1 / \partial t + \boldsymbol{v}_0 \cdot \nabla \rho_1 + \boldsymbol{v}_1 \cdot \nabla \rho_0 + \rho_0 \nabla \cdot \boldsymbol{v}_1 = 0, \tag{3}$$

$$\rho_0 \left[\partial \boldsymbol{v}_1 / \partial t + \left(\boldsymbol{v}_0 \cdot \nabla \right) \boldsymbol{v}_1 + \left(\boldsymbol{v}_1 \cdot \nabla \right) \boldsymbol{v}_0 \right] = -\nabla p_1 + \boldsymbol{J}_1 \times \boldsymbol{B}_0 + \boldsymbol{J}_0 \times \boldsymbol{B}_1 + \rho_1 \boldsymbol{g}, \tag{4}$$

where each variable is expressed as $\xi_0+\xi_1$ and index 1 denotes perturbations of steady state quantities (index 0). Usually, the incompressible assumption is used to simplify the derivation. However, it also makes the effects of the plasma compressibility and magnetic field undetectable. Considering the plasma temperature at the imploding stage we concerned is relatively low and the SAF velocities to be discussed are comparable to the local plasma sound speed, the plasma compressibility becomes an important role.

Assuming the perturbations vary as $\exp(-i\omega t+i\boldsymbol{k}\cdot\boldsymbol{r})$ and the wave vector $\boldsymbol{k}$ only has z component k, we can get the following second-order differential equation for the perturbed velocity v_{1x} (see Ref. [9] and [10] for detailed derivation):

$$\begin{aligned} & D\left[\frac{\rho_0 \left(\tilde{\omega} c_m^2 - k^2 V_A^4 / \tilde{\omega} \right) D v_{1x} + \rho_0 \left(k c_m^2 D v_0 - \tilde{\omega} g \right) v_{1x}}{\tilde{\omega}^2 - k^2 c_m^2} \right] \\ & + \rho_0 g \frac{\tilde{\omega} D v_{1x} + \left(k D v_0 - k^2 g / \tilde{\omega} \right) v_{1x}}{\tilde{\omega}^2 - k^2 c_m^2} + \left(\tilde{\omega} \rho_0 + \frac{g}{\tilde{\omega}} D \rho_0 \right) v_{1x} = 0, \end{aligned} \tag{5}$$

where $D = d/dx, \tilde{\omega} = \omega - k v_0$ is a Doppler shift applied to the perturbation frequency ω, and $c_m = (c_s^2 + V_A^2)^{1/2}$, c_s, V_A is the plasma magneto-acoustic speed, sound speed and Alfven velocity respectively. If the axial flow velocity v_0 is independent of x, the problem can be transformed to a frame of reference in which there is no equilibrium flow. Then, Eq. (8) can be reduced to the same as that with v_0=0.

The plasma slab is assumed to be surrounded by vacuums on both sides. To keep the pressure balance, the following condition should be satisfied at both plasma-vacuum surfaces

$$\boldsymbol{v}_1 \cdot \nabla \left(p_0 + p_{m0} \right) + d \left(p_1 + p_{m1} \right) / dt = 0, \tag{6}$$

where $p_{m0} = B_0^2/(2\mu_0)$, $p_{m1} = B_0 B_1/\mu_0$. Substituting parameters with v_{1x} into Eq. (6), the jump conditions become

$$x = -d: \quad \left[\left(\omega / k - v_0 \right)^2 - V_A^4 / c_m^2 \right] D v_{1x} + \left(\omega / k - v_0 \right) D v_0 v_{1x} = g v_{1x}, \tag{7}$$

$$x = d: \qquad \left(\omega / k - v_0 \right)^2 D v_{1x} + \left(\omega / k - v_0 \right) D v_0 v_{1x} = g v_{1x}. \tag{8}$$

Since equations (5), (7) and (8) contain no explicit time term, they should be satisfied with arbitrary disturbed velocity v_{1x}. These equations constitute an eigenvalue problem, which can be solved with a standard numerical technique such as shooting method. (Details of this numerical algorithm can be found in Ref. [11]) Unlike the case without flows, the perturbed velocity v_{1x} and the frequency ω are both complex, which means the real and imaginary part of the jump conditions should be satisfied synchronously.

In a previous paper[9] we have made a detailed discussion about the effect of plasma compressibility with various unperturbed states (incompressible uniform mass-density profile, compressible skin current profile and compressible uniform current profile). The main results of that study are as follows. The compressibility does decrease the growth rate of the KH instability, which is dominant at the small wavenumber region, in a Z-pinch imploding plasma, as well as works within the astrophysics frame. The contribution of the magnetic pressure to the plasma elasticity also becomes detectable in such a compressible model. Notice that c_m^2 in Eq. (5) can be presented as $dp^*/d\rho$, where p^* is the total pressure including a thermal part and a magnetic part. It reflects the resistance of the plasma to the deforming caused by outside force. If the plasma was disturbed perpendicularly to the magnetic field, the resistance of the frozen-in magnetic field is excited. As the wavelength decreases, perturbations get severe and magnetic field resists more powerfully. Because the sound speed embodies the plasma compressibility, people can analyze its effect by researching the effect of local sound speed. Fig. 2 shows the variation of the growth rate ($\Gamma = \mathrm{Re}(-i\omega) / (kg)^{1/2}$) as a function of the wavenumber ($K = 2dk$) with different sound speeds, which are calculated with a linear flow-profile whose peak velocity is 2×10^5m/s. The solid line corresponds to the result of incompressible case, $c_s \to \infty$. As the sound speed decreases, the mitigation effect on both the hybrid MRT/KH mode and MRT mode instability becomes efficient. As c_s=1×10^5 m/s with K=10, the growth rate is only about 40% of that of the case without SAFs. When the sound speed exceeds 8×10^5m/s (about 1keV for aluminum plasma), the compressible model result is close to the incompressible one. At the accelerating process of Z-pinch plasma, during which the kinetic energy is dominant, any kind of heating mechanism should be avoided. Therefore people usually choose heavy materials to keep the plasma temperature in a low range of 30-40eV [19], which corresponds to a sound speed less than 1×10^5 m/s. Therefore, on the early stage of the implosion, the compressible model is much more suitable and the mitigation effect of SAF performs much better than people estimated with an incompressible model.

3. Effect of Viscosity

The effect of the plasma viscosity is another important nonideal factor needed to be discussed. To analyze the viscosity effect, we have to go back to the basic functions of Eq. (1)

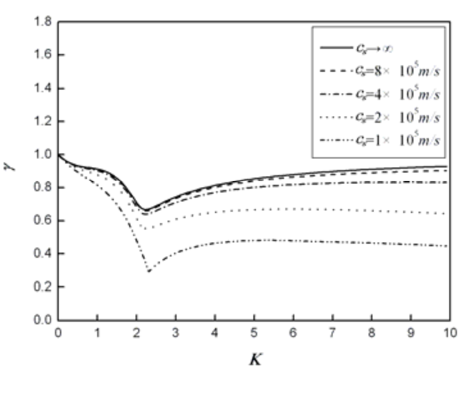

Fig. 2. Normalized growth rates vs. normalized wavenumber with different sound speeds .

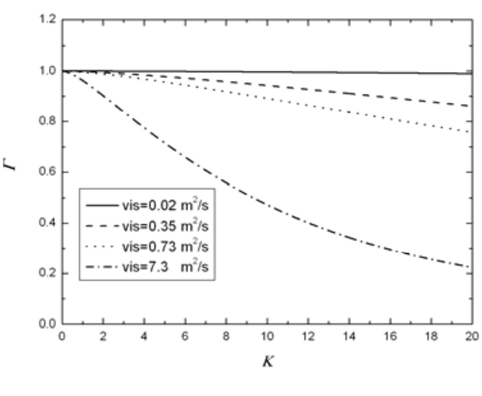

Fig. 3. Normalized growth rates vs. normalized wavenumber with various viscosity coefficients.

and Eq. (2). This time we neglect the effect of compressibility. Using the incompressible condition $\nabla\cdot\boldsymbol{v} = 0$, the perturbation equation derived from the motion equation and continuity function becomes

$$\tilde{\omega}\rho_0 v_{1x} + gD\rho_0 v_{1x}\tilde{\omega}^{-1} - i2D\mu Dv_{1x} - i\mu\left(D^2-k^2\right)v_{1x} = k^{-2}D\left[\tilde{\omega}\rho_0 Dv_{1x} + k\rho_0 v_{1x}Dv_0 - iD\mu\left(k^2+D^2\right)v_{1x} - kD\left(\mu Dv_0\right) - i\mu\left(D^2-k^2\right)Dv_{1x}\right], \tag{9}$$

where μ (which can be a function of x) denotes the coefficient of viscosity.

To get proper jump conditions at the interface between two fluids, it's necessary to specify which quantities should be continuous at the interface. Clearly, the velocity, as well as the tangential viscous stresses, must be continuous. The continuity of Dv_{1x} follows from incompressible condition and the continuity of v_{1y} and v_{1z}. To ensures the continuity of the tangential viscous stresses, it's easy to get the condition that $ik\mu Dv_0 - \mu(D^2+k^2)v_{1x}$ must remain continuous across an interface. Integrate equation (14) over an infinitesimal element of x including the interface, we get the jump condition

$$k^2 g\Delta\left[\rho_0\right]v_{1x}\tilde{\omega}^{-1} - i2k^2\Delta\left[\mu\right]Dv_{1x} = \Delta\left[\tilde{\omega}\rho_0 Dv_{1x} - i\mu\left(D^2-k^2\right)Dv_{1x} - iD\mu\left(k^2+D^2\right)v_{1x} - k\left(D\mu Dv_0 + \mu D^2 v_0 - \rho_0 v_{1x}Dv_0\right)\right], \tag{10}$$

where $\triangle[f] = f_{x+} - f_{x-}$. For simplicity, we set the plasma density and viscosity are uniform and the SAF has a linear profile: $v_0=V_0(1-x/d)/2$. Therefore the disturbed velocity equation and interface conditions can be simplified to

$$k^2\left[\tilde{\omega}\rho_0 v_{1x} - i\mu\left(D^2-k^2\right)v_{1x}\right] = D\left[\tilde{\omega}\rho_0 Dv_{1x} + k\rho_0 v_{1x}Dv_0 - i\mu\left(D^2-k^2\right)Dv_{1x}\right], \tag{11}$$

$$\begin{aligned} x=\pm d \qquad & v_{1x} = v_{1x=\pm d}, \quad Dv_{1x} = \mp kv_{1x=\pm d}, \\ & \left(D^2+k^2\right)v_{1x} = -ikV_0/2d, \\ & \gamma D^3 v_{1x} + \left(i\omega - ikV_0 - 3\gamma k^2\right)Dv_{1x} - ik^2 g v_{1x}\left(\omega - kV_0\right)^{-1} + ikv_{1x}Dv_0 = 0, \end{aligned} \tag{12}$$

where we used the general solution formats $v_{1x}\sim e^{\pm kx}$ at the vacuum region. Equation (11) and corresponding boundary conditions (12) constitute the formulation of the linearized stability problem as an eigenvalue problem. Since ω enters Eq. (11) in a complicated nonlinear way, it has no analytical general solutions. To gain an analytical dispersion relation, we make $V_0 = 0$ to simplify such a SAF question to a case without axial flow and Eq. (11) degrades to

$$\left(D^2-k^2\right)\left[1 - i\gamma\left(D^2-k^2\right)\omega^{-1}\right]v_{1x} = 0, \tag{13}$$

where $\gamma\,(=\mu/\rho)$ is the coefficient of kinematical viscosity. The general solution of Eq. (13) is a linear combination of the solutions $e^{\pm kx}$ and $e^{\pm qx}$, where $q = (k^2-i\omega/\gamma)^{1/2}$. Substituting them into Eq. (13), the corresponding boundary conditions can be rewritten in matrix notation, and we essentially gain the analytical dispersion relationship

$$8k^2\gamma^4 q\left\{q\left(3k^4+q^4\right) - \left[cth\left(2dk\right)cth\left(2dq\right) - 4\operatorname{csc}h\left(2dk\right)\operatorname{csc}h\left(2dq\right)\right]k\left(q^2+k^2\right)^2\right\} + n^4\left[1-\left(kg/\omega^2\right)^2\right] = 0, \tag{14}$$

where it may be recalled that q_2 are related to ω. If the plasma has no viscosity, it has a solution of $\omega = i(kg)^{1/2}$, which corresponds to the RT instability of an ideal case. Considering the complexity of Eq. (14), it's instructive to study the asymptotic behavior of ω for $k\to0$ and $k\to\infty$. The dispersion relations for these two limits becomes

$$\omega \to i\sqrt{kg} \qquad (k\to 0), \tag{15}$$

$$\omega \to ig/2k\gamma \quad (k\to\infty). \tag{16}$$

The asymptotic relation for $k\to0$ is exactly that which obtains in the absence of viscosity. This agreement shows that viscosity plays no role among the very long wavelengths. According to equations (15) and (16), $\omega\to0$ both when $k\to0$ and $k\to\infty$. Therefore there exists a mode of maximum instability. With the parameters we used before, the (Γ, K) relationships calculated numerically are illustrated in Fig. 3. The four curves correspond to γ= 0.02, 0.35, 0.73, and 7.2 m^2/s respectively (relevantly, the tungsten ion temperature T_i=0.6, 2, 2.6, and 6 keV), which have been used in reference [12]. In the wavelength region we are concerned, the mitigation effect, which is also suspect to the magnitude of the viscosity, enhances as the wavenumber increases. When the viscosity approaches to 7.2m^2/s, corresponding to a high plasma temperature about 6 KeV, it gives a sufficient mitigation to the growth rate about 80%. But during the accelerating process the plasma temperature usually keeps in a low range about 30-40eV. Therefore, according to Fig. 3, the mitigation effect of viscosity is slight enough to be omitted. Although the results presented here suggest that, the viscosity seems insignificant to the growth rate, it doesn't mean that the viscosity isn't important to the Z-pinch implosion. Some researchers have pointed out the plasma viscosity may play a crucial role in the energy transition process because of its inherent relationship with anomalous heating mechanism.

It's important to note that the upper conclusion is based on a simplified model without SAF. As the combination terms of viscosity and SAF exist in the disturbed velocity equation and interface conditions, it is necessary to take the combination effect of these two factors into consideration when SAFs are introduced. The magnitude of such a hybrid effect, which we are interested in and working at, should be directly calculated from Eqs. (11), and (12) numerically.

4. Effects of Different Flow Profiles

Nowadays, the upper limit of the practical peak velocity of axial flows is about 1~1.5 Mach, which suggests that it's difficult to improve the stability via increasing the axial flow's peak velocity, and the analysis of different flow profiles becomes necessary. Based on a uniform current model which is compressible but not viscous, we investigated the effects of the following exponential profiles:[10]

$$v_0 = \begin{cases} V_0\left[(1-x/d)/2\right]^{\alpha} & \alpha = 1,2,3, \\ V_0\left[(1+x/d)/2\right]^{\beta} & \beta = 1,2,3. \end{cases} \tag{17}$$

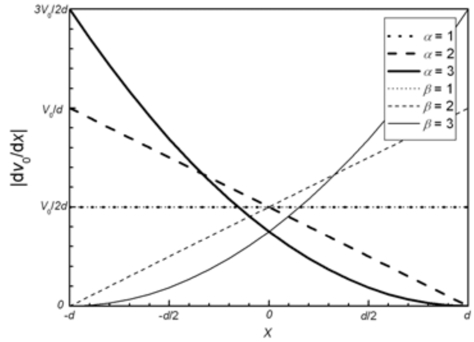

Fig. 4. The velocity shear distributions of different flow profiles.

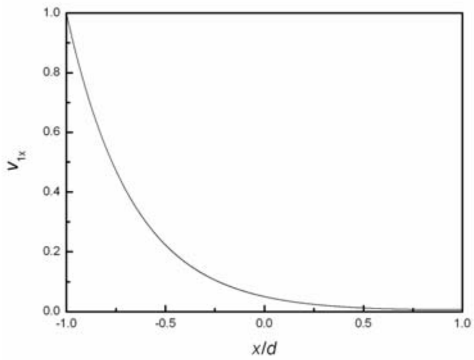

Fig. 5. The general distribution of the perturbed velocity v_{1x}.

Distributions of velocity shears and a typical profile of the disturbed velocity v_{1x} are shown in Fig. 3 and Fig. 4 respectively. It's easy to find out the velocity shears of α– and β– profiles are symmetrical with $x = 0$, and the $\alpha = 3$ case has the most similar curved shear profile with the distribution of the disturbed velocity.

Numerical results of different flow profiles with $V_0 = 2\times10^5$ m/s are shown in Fig. 5. The diverse mitigation effects show that, when the peak velocity keeps unchanged, the value and the distribution of the velocity shear become the crucial factors. The α-profiles, whose peak shears concentrate at the outer edge, perform much better than β-profiles. Especially the $\alpha = 3$ velocity profile presents the best mitigation effect, and the suppressed growth rate is only about 35% of the case without flows at $K = 9$. Comparing the two cases of $\alpha = 3$ and $\beta = 3$ we find that the mitigation effect on the MRT instability, which is performed by the velocity shear, is highly susceptible to the magnitude of the shear nearby the outer plasma surface. It is known that the MRT instability develops at the interface between the plasma and the magnetic field. According to the Z-pinch plasma, perturbations concentrate at the outer surface ($x = -d$), so the magnitude of the flow shear at the outer interface is critical to sustain stability. Therefore, within the practical velocity limitation, it's possible to promote the mitigation effect markedly by constructing a suited flow profile.

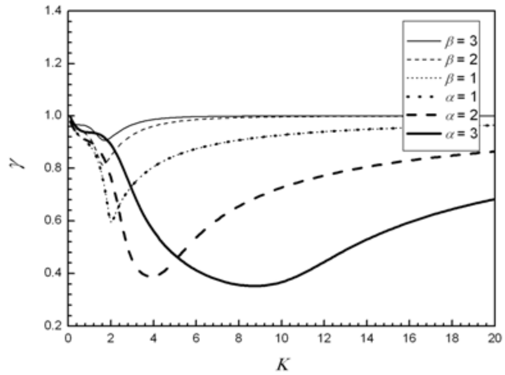

Fig. 6. The normalized growth rates γ vs. normalized wave number K with different flow profiles.

5. Conclusions

The effects of two nonideal factors, compressibility and viscosity, on the MRT instability in Z-pinch implosions have been discussed within the magneto-hydrodynamic (MHD) frame. The plasma compressibility is demonstrated to be important on estimating the stabilizing effect of the SAFs, especially during the linear developing phase of the RT instability. On the one hand, the plasma compressibility debases the growth rate of MRT/KH mode. On the other, the effect of the magnetic pressure can be reflected in such a compressible system. The effect of the plasma dynamic viscosity in a case without SAFs seems neglectable as the plasma temperature is relative low, less that 100eV, but the coupling effect with the SAF in an axial flow introduced system should be calculated seriously. We have presented the self-contained equations to such a question, and will working on it later.

Various flow profiles are also discussed in this paper. Results presented here suggest that, the mitigation effect of the axial flow on the MRT instability is highly susceptible to the magnitude of the velocity shear nearby the plasma outer surface (the interface between the plasma and the magnetic field), and the mitigation performance can be promoted markedly by constructing a suited flow profile. This inspiring result reminds that, when using sheared axial flows as a stabilizing method, people should not only increase the peak velocity, but also optimize the velocity profile to make the velocity shear concentrates at the outer surface and get the best mitigation effect.

Acknowledgments

The authors wish to acknowledge the Z-pinch research team of IAPCM and Prof. Ding Li and Prof. Wen-Hua Ye for their helpful discussions.

References

[1] Deeney, C., et al., Phys. Rev. Lett. **81** (1998) 4883.
[2] Sanford, T.W.L., et al., Phys. Rev. Lett. **77** (1996) 5063.
[3] Shumlak, U., Hartman, C. W., Phys. Rev. Lett. **75** (1995) 3285.
[4] Arber, T.D., and Howell, D. F., Phys. Plasmas **3** (1995) 554.
[5] Shumlak, U., et al., Plasmas **10** (2003) 1683.
[6] Shumlak, U., Roderick, N. F., Phys. Plasmas **5** (1998) 2384.
[7] Ong, R.S.B., Roderick, N., Planet. Space Sci. **20** (1972) 1.
[8] Kubes, P., et al., IEEE trans. Plasma Sci. **22** (1994) 986.
[9] Zhang, Y., Ding, N., Phys. Plasmas **13** (2006) 022701.
[10] Zhang, Y., Ding, N., Phys. Plasmas **13** (2006) 062703.
[11] Kincaid D., Cheney W., *Numerical Analysis: Mathematics of Scientific Computing, Third Edition*, (Wadsworth Group, 2002) p581.
[12] Qiu, X.M., et al, Chin. Phys. Lett. **21** (2004) 689.